Astro. Lett. and Communications, Vol. 37, pp. 205–217
Reprints available directly from the publisher
Photocopying permitted by license only

The PLANCK LFI Radiometer – Prototype Results

Philip Lubin, Peter Meinhold and Jeffrey Childers
Physics Department
University of California, Santa Barbara
Santa Barbara, CA 93106
805-893-8418

ABSTRACT

The Planck LFI (Low Frequency Instrument) will consist of a focal plane array of cryogenically cooled High Electron Mobility Transistor (HEMT) receivers operated in a differential mode to continuously compare the sky beam to a cryogenic reference load. The baseline design for this receiver is a pseudo-correlation or continuous comparison radiometer, the design of which has been optimized for reduction of 1/f type noise, high bandwidth, and high sensitivity. As part of our effort, we have built a prototype receiver operating near 40 GHz in order to design, test and investigate important tradeoffs in optimizing the system. The prototype receiver is an important step in proceeding to the flight design and allows us to rapidly test ideas on the front end through the detectors, DC signal processing, and data acquisition. We have achieved a knee frequency of 10 mHz with a bandwidth of 2 GHz. We will discuss the rational for the receiver design and some of the tests and limitations we have encountered as well as the future plans.

Keywords: Cosmic Microwave Background, Cosmology, Radiometry

1. INTRODUCTION

The Planck mission goal of producing near full sky maps with low residual instrumental contamination and stripping leads to strict requirements on the instrumental stability on long time scales. To insure that information is preserved on low as well as high spatial frequencies we will need to have detectors with stability comparable to the spacecraft

spin rate (≈ 0.01 Hz). Both the HFI and LFI have similar stability requirements though the method of stabilization is radically different. The LFI is consists of a focal plane array of differential High Electron Mobility Transistor (HEMT) amplifier based receivers operating in bands near 30, 44, 70 and 100 GHz. With a scan strategy consisting of circular scans with little or no interconnections between scans except at the "polar" crossings, it is critical that the instrumental stability be long or else significant "map stripping" can result. In the end, it is possible that we can live with a relaxed requirement on stability if robust reconstruction techniques can be developed. This is an important question that needs to be explored further by doing detailed mission simulations with various receiver stabilities.

All real detectors exhibit some form of time dependent "drift" normally taking the form of a gain variation or a noise variation or often both. HEMT's exhibit gain instabilities which in general are worse in small gate length devices. With gate lengths of order 0.1 microns and gate widths of a few tens of microns and ariel current densities of about $3x10^{12}$ e-/cm^2 the total charge in the gate is only about 10^4-10^5 electrons. This small number of electrons interacting with channel defects, traps, $\sqrt{N}$ fluctuations and likely other currently unknown factors, can lead to significant amplifier fluctuations which have a nearly "1/f" spectrum that is so ubiquitous in detectors. We will define the 1/f 'knee' frequency f_k to be the frequency at which the noise contribution from the amplifier instability is equal to the white noise, which is the noise in high frequency limit. Our and other researchers experience to date shows that this effect is worse in higher frequency amplifiers, worse in InP versus GaAs and increasingly problematic at lower temperatures. Figure 1 shows a typical HEMT noise power spectrum taken in our lab at 40 GHz using a 5 stage amplifier with the first stage being an InP device and the latter stages GaAs. Note the rapid increase below 10Hz. The amplifier was cooled to 4 K for this test.

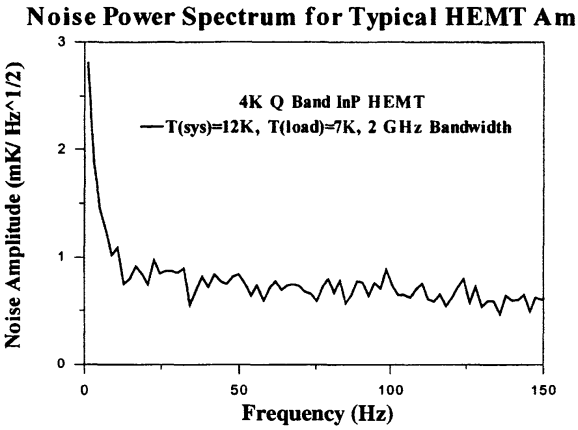

As can be seen this amplifier has a f_k of about 30 Hz or about 2000 times the spacecraft spin frequency, assuming a 1 RPM spin rate (16 mHz). This is clearly unacceptable in a detector for the Planck mission. A similar problem existed for the COBE DMR experiment as well as many of the other ground based and balloon borne experiments we have pursued. This is a common problem in radiometry and not unique to CMB detectors. Classically, this problem is overcome by switching the input signal and differencing it against either another similar signal (as in COBE for example) or against an artificial signal such as a noise source. By differencing two signals which are near in amplitude to each other, gain fluctuations acting on the difference which can be made very small by proper balancing and matching. This assumes we can switch at a rate rapid compared to the gain fluctuation rate i.e. $>>f_k$. The input signal can be switched by a variety of techniques including mechanical switches, beam chopping techniques, Ferrite or semiconductor switches (Dicke switch) or by a interferometric or a correlation technique. The latter is the baseline design for the Planck LFI.

The baseline receiver design for LFI is of the 'pseudo-correlation' or 'continuous comparison' type, which has been used for over 30 years (Blum 1959, Colvin 1961, Faris 1967). Detailed discussion of the reasons for choosing this design and a theoretical exploration of it's fundamental operation can be found in Bersanelli et al, 1996, and Seiffert at al, 1998. A schematic diagram of the receiver planned for the Planck LFI shown in Figure 2.

The radiometer works by passing the input signals (Antenna = amplitude x, Reference = amplitude y) into a 180 degree hybrid (or "magic tee") that then outputs x+y and x-y to the corresponding amplifiers. Ignoring the Phase Shifters (φ) for the moment we see that the second hybrid (same design as the first) simply reverses the process and ideally outputs the amplitudes $G_c\,(x+y) + G_c\,(x-y) = 2G_c\,x$ and $G_c\,(x+y) - G_c\,(x-y) = 2G_c\,y$. In other words, ignoring the factor of two in amplitude and voltage gain of the amplifier (assumed equal here) G_c (c for cryogenic), we just end up with the Antenna and Reference Load, x and y

respectively. This seems like a lot of work to end up with what we started with. Why do we do this? The reason is that the cryogenic amplifiers act on x+y and x-y not just x and y individually. Further amplification through the warm amplifiers (gain G_w) just increases the amplitude further. The rectification stage ("detector diodes" in Figure 2) puts out a voltage proportional to the squares of the input and after differencing we get and output voltage equal to $4\alpha(G_c\ G_w)^2\ (x^2 - y^2)$ where "α" is the diode conversion (assumed to be equal in both diodes) of volts out per watt in. Note that x^2 and y^2 are just proportional to the power inputs and in the low frequency limit to the input radiometric temperatures. Hence, in the end the radiometer outputs a voltage proportional to the temperature difference between the antenna (sky) and the Reference Load amplitudes. This is just what we want to reduce the effects of the HEMT amplifier gain variations. A more detailed analysis is given in Seiffert et al 1998 and includes many of the non-ideal characteristics we encounter in a real system.

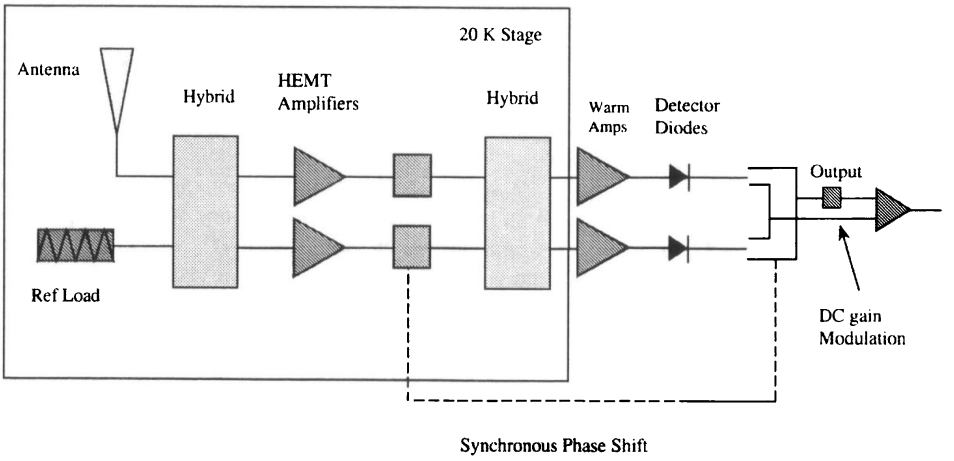

Figure 2: Schematic diagram of the baseline LFI receiver. As mentioned below the 40 Ghz prototype design is slightly different to allow for more flexibility in testing. In particular we do not use the last differential amplifier but rather sample the diode outputs directly and perform the differencing in software.

2. THE LFI PROTOTYPE RADIOMETER AT 40 GHZ

As part of the US role in the Planck LFI we are prototyping a receiver at 40 GHz. The principal goal in building the prototype is to test the baseline design and optimize the design as necessary. We are also testing a number of issues related to the stability of the instrument, the data acquisition system and the dependence on the temperature and design of the cold load. In addition, we would like to investigate the sensitivity of the system to various systematic effects, such as temperature drift in backend components etc. In this process we have already gained important information that will feed into the design of the next breadboard at 100 GHz being built at JPL.

3. RADIOMETER CONSTRUCTION

Figure 3 shows the layout of our test radiometer, constructed largely of parts from our balloon programs. Figure 4 shows a picture of the actual test radiometer. We cool the cryogenic portion of the radiometer to 4 K with a liquid Helium. There are a few differences between Figure 2 and Figure 3. We are using only 1 phase shifter. The second hybrid is warm, and we have inserted variable attenuators in each leg. This allows us easy access to the phase matched legs of the radiometer, primarily in order to perform gain match using the amplifier bias and an attenuator, and phase match using shims at the wave-guide interfaces. One input is coupled to a temperature controlled wave-guide load, the other is coupled to an identical load with a cross-guide coupler. The cross-guide is realized in stainless wave-guide for thermal isolation between the cold radiometer and the warm section, and provides a –38 dB coupling value to a vacuum feed-through, used to inject signals from the vector network analyzer (HP 8510C). This input configuration allows us to tune the gain and phase match with the network analyzer with the system cold. When we remove the analyzer we can then operate the radiometer with the controllable thermal loads to investigate noise and stability at different load temperatures and temperature differences.

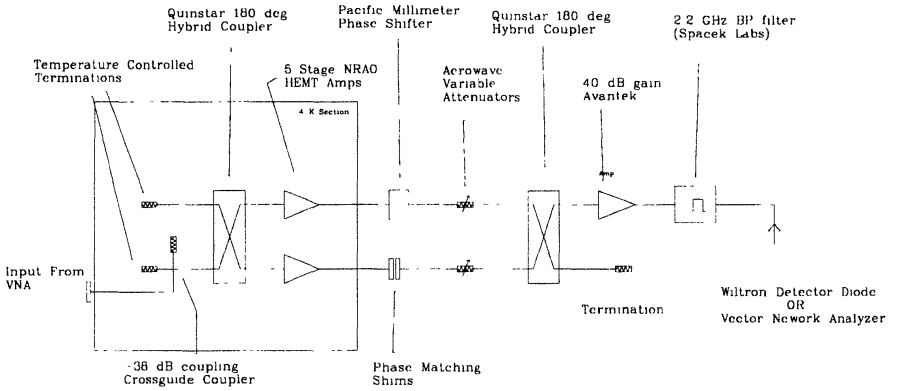

Figure 3. Schematic of the Prototype Radiometer. Note differences from Figure 2, particularly division of phase sensitive section between warm and cold parts, and the low coupling value cross-guide at one input for VNA signal injection.

UCSB 44 GHz Test Radiometer

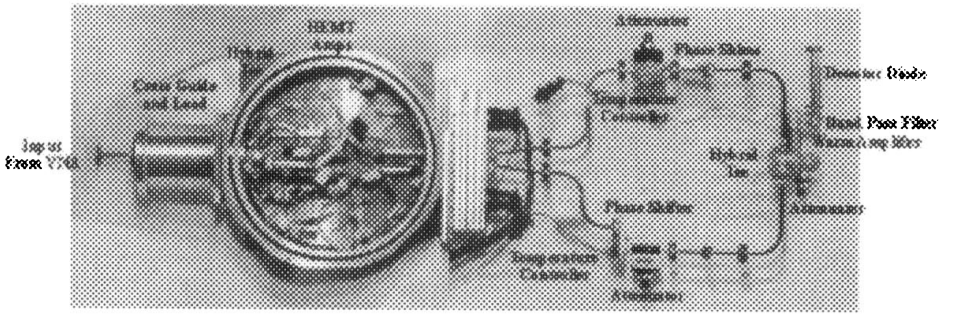

Figure 4. View of the 40 GHz prototype from the bottom. (See Color Plate V).

The cryogenic amplifiers currently being used are an based on NRAO design, constructed with discrete devices: 1 stage of InP HEMT from Hughes, 4 stages of GaAs HEMT from Starcomm. The 180 degree hybrid couplers are from Quinstar and the 0/180 degree phase switch is from Pacific Millimeter. The detector diode is a Wiltron 75KC50, and the attenuators are from Aerowave. The warm amplifier (from Avantek) has a gain of approximately 40 dB, and we have a 2.2 GHz wide waveguids iris filter from Spacek Labs. We use this filter to define our bandwidth, and to give us a smaller range over which to match our two amplifiers (as the amps were not expressly designed to be identical). The input terminations are made of Eccosorb (CR117), machined to a very fine point and inserted into stainless steel waveguide sections. A small temperature sensor is inserted directly into the Eccosorb, and the temperature of the load is determined by balancing cooling from a copper strap to the 4 K plate with input power to a heater resistor attached to the load. The loads have better than –35 dB return loss. The cross guide coupler and precision cold load are shown in Figure 5.

We now generalize the analysis slightly by allowing different gains and noise temperatures in the two cold amplifiers. The voltage measured at each of the two detector diodes is of the form:

$$V_d(t) = \frac{a}{2}\left[\left(\frac{x+y}{\sqrt{2}} + n_1\right)g_1 \pm \left(\frac{x-y}{\sqrt{2}} + n_2\right)g_2\right]^2$$

44 GHz Cross Guide Coupler and Load

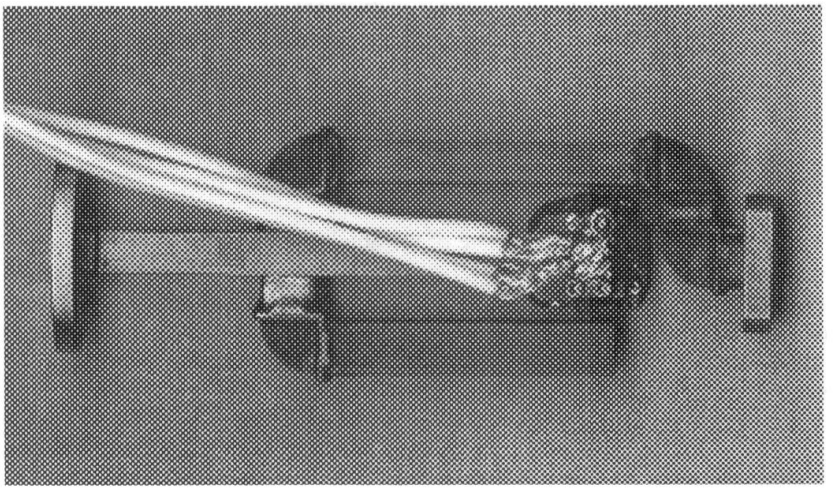

Figure 5. Cross guide coupler and precision cold load. (See Color Plate VI).

Here, x(t) is the noise voltage at the sky horn (antenna) , y(t) is the noise voltage of the reference load, $n_1(t)$ and $n_2(t)$ are the noise voltages contributed by the amplifiers, g_1 and g_2 are the voltage gains of the two amplifiers, the plus(minus) sign indicates 0 or 180 degree net phase shift from the phase shifter, and the diodes are assumed to be perfect square law detectors with a constant of proportionality of "a". Note that the two diodes are complementary, with a fixed net phase shift of 180 degrees. When the gains g_1 and g_2 are matched, and assuming $n_1=n_2$ for simplicity, we obtain:

$$V_d(\Phi=0) = ag^2(x^2 + \frac{n_1^2 + n_2^2}{2})$$

and

$$V_d(\Phi = 180) = ag^2(y^2 + \frac{n_1^2 + n_2^2}{2})$$

Where we have now ignored cross terms in noise voltage, since they are assumed to be uncorrelated and average to zero. Noting that here $x^2=kT\beta$, in the Rayleigh Jeans limit we can cast this result in terms of the input temperature to get :

$$V_d(\Phi = {}^{0}\!/_{180}) = ak\beta g^2(T_{{}^{x}\!/_{y}} + T_n)$$

Here, T_n is the average noise temperature of the amplifiers, β is the effective bandwidth, k is Boltzmann's constant. Thus the output of the radiometer in each phase switch state reflects the temperature at one of the inputs in addition to the average noise temperature of the amplifiers. In the case of the LFI, one input will be directed at the sky through the telescope, while the other will connected to a termination. To use this topology as a differential radiometer, we may either difference the outputs of the two diodes, or we may modulate the phase switch at a high rate (500 Hz or more) and difference successive measurements of each diode. In either case, in order to null the system and minimize the 1/f noise contribution, we need to multiply one of the states by a constant, shown (Seiffert 1998) to be:

$$r = \frac{T_x + T_n}{T_y + T_n}$$

We have chosen to use successive differences on each diode, minimizing the 1/f contributions of the detector diodes, warm amplifiers, and reducing our sensitivity to back end temperature gradients etc.

Thus our final radiometer output looks like:

$$V = V_d(\Phi = 0) - rV_d(\Phi = 180) \propto T_x - T_y$$

In practice, we perform this difference in software, giving us more control over the value of r, and information about the 1/f characteristics of the individual phase states before differencing. Seiffert (1998) gives an expression for the 1/f knee frequency of the radiometer:

$$f_k = \frac{A^2\beta}{8}(1-r)^2\left(\frac{T_n}{T_n+T_x}\right)^2$$

A is a number describing the intrinsic stability of the amplifiers, and has a value of $1.8\text{x}10^{-5}$ for the 5 stage 44 GHz amplifiers used.

4. SYSTEM TUNING

In order to tune the phase and gain of each leg in the system we hook out radiometer up to a vector network analyzer (VNA). This is done by first biasing only one of the cold HEMT amplifiers and measuring the system gain. Then we bias only the other amplifier and measure the gain difference. By tuning bias settings and attenuation in the two legs, we can generally get the gain matched within 1 dB across our 2.2 GHz band-pass. The same procedure is then followed for the phase match, where tuning is accomplished by inserting shims of different thickness at a wave-guide joint in one leg of the radiometer. Phase match across the band of ±10 degrees is relatively easy to obtain. The next step is to measure the 'isolation' of the system, where we measure the difference between the radiometer output in the phase state looking at the termination, and the output while looking at the VNA. This is indicative of the overall gain/phase match of the system, generally we achieve between –20 and –25 dB isolation.

5. DATA ACQUISITION SYSTEM

To allow maximum flexibility in the analysis of the radiometer we sample the diode output directly and do not use a hardware differential amplifier. For the flight version of the system it is quite possible that we will proceed on the same path as this gives us flexibility to do software signal processing using a DSP. We therefore require high gain, large dynamic range and sampling synchronous with the phase switch state. We typically sample at 1 kHz, and switch the phase at 500 Hz. The analog section consists of a x10 low noise preamp, a switchable gain stage (x1-x100) followed by a dc offsetting circuit. We minimize the DC component of the signal going into the integrator to increase our dynamic range. The integrator is followed by a sample and hold circuit. The output of the sample and hold and the preamp section are brought out through linear opto-isolator amplifiers. A separate timing board synchronizes the sample and hold and integration/reset in addition to the phase switch signal. In general, the gain switching in the second stage of pre-amplification is used to set the dynamic range rather than to null the output as we have been able to do the nulling in software. The procedure is to acquire 600+ seconds of data sampled at 1 kHz, then to separate out the 0 phase state samples from the 180 phase state samples. We then calculate power spectra for these data sets and find the value of r by comparing the white noise levels. The white noise of the detector in a given phase switch state is given by:

$$\Delta T = \sqrt{2}\frac{(T_s + T_n)}{\sqrt{\beta\tau}}$$

which is a modification to the standard radiometer equation, including an extra factor of $\sqrt{2}$ due to the 50% duty cycle of one switch state. Thus r is equal to the ratio of the white noise levels in the individual phase states. We previously used AC coupling between the preamp and the integrator to increase our dynamic range, but found that in order to properly calculate and apply the correct value of r, it was necessary to replace the AC coupling with a DC offset circuit. Unless the AC time constant is longer than the time-scale of interest (i.e. 100 seconds or so), information will be lost, and the subtraction will be incorrect on time-scales longer than the coupling time constant. A picture of the prototype data acquisition system is shown in Figure 6.

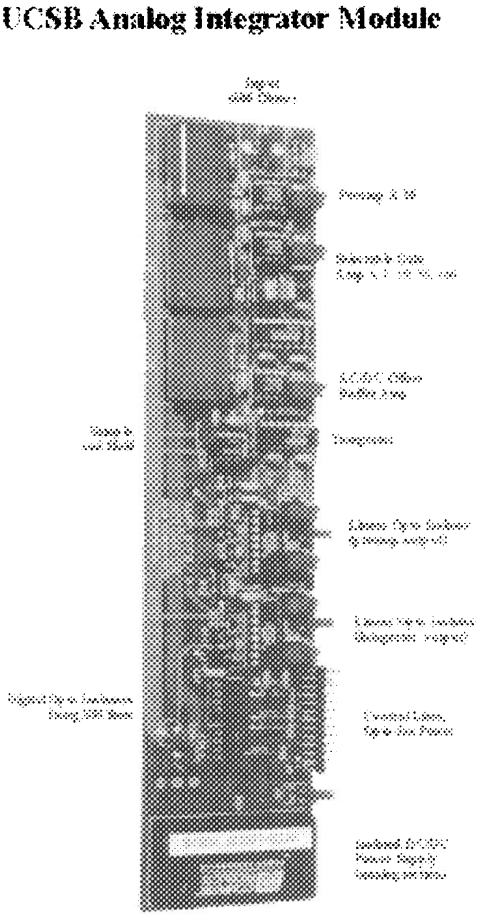

Figure 6. Prototype LFI post detector analog data processing module. (See Color Plate VII).

6. RESULTS

Figure 7 shows the power spectra from the two phase states superimposed, in the case of a (relatively large) offset of 13 K as well as the power spectrum of the difference. Note that we generally plot the square root of the power spectrum (V/√Hz).

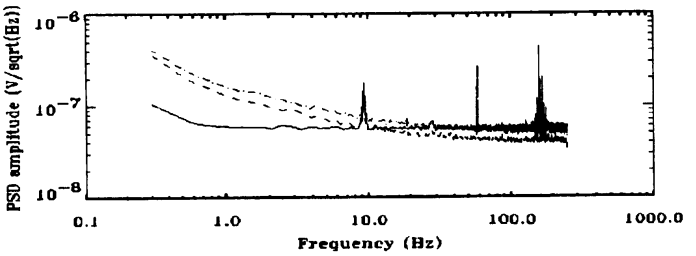

Figure 7. Power spectra of the diode output in the two phase states as well as difference between the two states for a 13 K temperature difference. The dash-dot line is for the phase viewing the 20 K termination, the dash line is the phase viewing the 7 K termination, and the solid line is the difference data. The effective knee frequency for the undifferenced data is around 10 Hz.

Calibrating the system in temperature units instead of voltage units we find from the white noise limits white noise an amplifier noise temperatures of around 40 K and noise consistent with our bandwidth of 2.2 GHz. The load temperatures used in the above plot are 20 K and 7 K. Figure 8 shows an expanded plot of the power spectrum of the difference data set from Figure 7, in addition to a difference power spectrum from a data set with offset smaller than 1 K. The difference in the knee is evident, particularly from the fits, which give 30 mHz for the 13 K offset curve and 12 mHz for the 1 K offset.

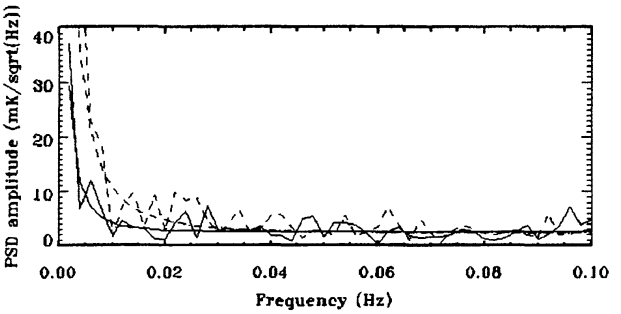

Figure 8. Expanded view of the differenced data of Figure 7 with linear axes and temperature along the vertical axis. The solid line is for e small offset (≈1K) and the dotted line is for larger (13K) offset case along with fitted curves. Fits are nearly 1/f though not precisely.

Perhaps the most striking illustration of the capability of the radiometer is given in Figure 9 where we have plotted the time series of the two phase-shift states as well as the difference data. It is clear from the difference data that the two phase shift states are well correlated and allow an excellent subtraction to be done.

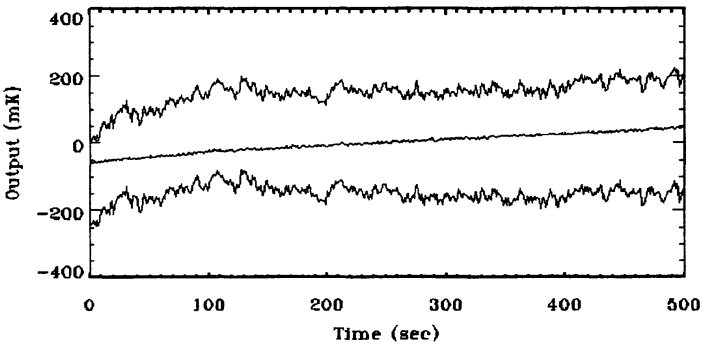

Figure 9. Time series of data for the two phase shift states and difference. Note the very significant reduction in noise in the difference data. Terminations were within 1 K (close to the expected on-orbit case) of each other for this test.

7. DISCUSSION

While these results are extremely encouraging how do they compare to the ideal system? We calculated above the relation between 1/f knee frequency and system parameters. If we use the 13 K temperature difference case shown above, we would expect f_k~1 mHz for the 13 K offset case, and correspondingly less for the low offset (1K difference) case. The reasons for not reaching the theoretical numbers are not fully understood though not completely unexpected. Such long time scales of 1/f knees near 10 mHz require exceptional stability on all aspects of the system. The prototype is not expected to be stable on extremely long time scales due to it nature as a rapid prototype system. The fact that we are already achieving the 10 mHz stability we would like to see for the flight system is very encouraging but we would like to understand what is actually limiting us. As we increase the bandwidth we expect the intrinsic 1/f knee frequency to increase proportional to bandwidth β. This is one of our next tasks to explore. If we can keep the 1/f knee to 10 mHz with bandwidths near 10 GHz we will very close to the needs for the flight system. In the flight configuration, all of the phase sensitive parts will be in a single housing, cooled to 20 K and kept far more thermally and mechanically stable than we can achieve with our current setup, so our results allow us to be very optimistic. In addition there is some evidence that our phase shifter may be the limiting element in the prototype. Tests done on the phase shifter stability alone indicate that the differential loss may vary by several parts in 10^5 on a time scale of 100 seconds (10 mHz). The phase shifter design we are using for the prototype will be changed for flight as we will try to use a baseline cryogenic phase shifter.

8. CONCLUSION

We have demonstrated excellent stability in the 40 GHz prototype LFI radiometer. We have developed a data acquisition system that meets the needs of a prototype system. We have identified a number of areas of concern and will be testing several ideas for optimization in the next year of work.

REFERENCES

1. Bersanelli et al., 1996. *ESA, COBRAS/SAMBA Report on the Phase A Study,* D/SCI(96)3.
2. Blum, E. J., 1959, *Annales d'Astrophysique*, 22-2,140.
3. Colvin, R.S., 1961, Ph.. Thesis, Stanford University.
4. Faris, J.J., 1966, *J. Res NBS*, **71C**, No. 2, 153.
5. Seiffert, M. et al, *Rev. Sci. Instrum.*, submitted 1997.